3D 360° surface morphometric analysis of pounding stone tools used by Hadza foragers of Tanzania: a new methodological approach for studying percussive stone artifacts

Alfonso Benito-Calvo[1*], Alyssa N. Crittenden[2], Sarah V. Livengood[3], Laura Sánchez-Romero[1,4], Adrián Martínez-Fernández[1], Ignacio de la Torre[5], Michael Pante[6].

[1] CENIEH. Paseo Sierra de Atapuerca 3, 09002 Burgos, Spain

[2] Department of Anthropology, University of Nevada, Las Vegas, Las Vegas, Nevada 89154, USA

[3]Department of Anthropology, University of Arkansas, Fayetteville, Arkansas, 72701, USA

[4] Doctorado Interuniversitario de Evolución Humana, Paleoecología del Cuaternario y Técnicas Geofísicas Aplicadas a la Investigación, Universidad de Burgos, Juan de Austria 1, 09001 Burgos, Spain.

[5] Institute of Archaeology, University College London, 31-34, Gordon Square, WC1H 0PY

London, United Kingdom

[6] Department of Anthropology, Colorado State University, Fort Collins, Colorado, 80523, USA

*Corresponding author: Alfonso Benito-Calvo. CENIEH, Paseo Sierra de Atapuerca 3, 09002 Burgos, Spain. Email: alfonso.benito@cenieh.es

Abstract

Surface morphometry comprises a relevant set of techniques that provide objective tools to identify, map, and understand use wear patterns in stone tools. Thus far, these techniques have been applied mainly to 2D or 2.5D data, but their application to 3D 360° data is promising and still underdeveloped. Here, we apply new 3D techniques to calculate morphometric variables and to analyse surficial features and changes in pounding stone tools used for baobab processing among Hadza foragers of Tanzania. Baobab pounding stones were collected after use by Hadza foragers for processing the plant food and then 3D point clouds were acquired from laser scanners and SfM photogrammetry. Morphometry was conducted directly on 3D point clouds to avoid time-consuming and surface modifications related to more complex 3D data, such as meshing. Several morphometric variables were computed for the complete pieces (360°

sphere) providing fast and accurate data to identify the detailed morphometric features of the artefacts. Additionally, stone surface changes due to baobab processing were measured by comparing the stone surface before and after use, thus enabling calculation of spatial abrasion patterns. Data were interpreted using multivariate exploratory statistical analysis. Differences in the effect of processing on surface morphology are likely explained by variations in raw source material and use. Results suggest that the traces produced by baobab processing on stone tools should be detectable in the archaeological record.

Keywords: 3D surface morphometry, pounding stone tools, use wear, baobab processing, multivariate exploratory statistics

1. Introduction

The use of pounding tools to process plant foods is a common behavior among extant primates, contemporary foragers, and in the archaeological record (de la Torre and Hirata, 2015). Traces of pounding activities in the form of pitted hammerstones and anvils appear early in the archeological record, suggesting pounding had an important role in hominin food processing behavior and ultimately may have contributed to the emergence of stone tool knapping (Marchant and McGrew 2005; Mora and de la Torre 2005). Despite their significance, few attempts have been made to quantitatively study use wear of battered objects used in various food processing techniques (Arroyo et al. 2016; De la Torre et al. 2013). As our understanding of the significance of plant foods in hominin evolution increases (Hardy and Martens 2016; Henry et al. 2014; Schnorr et al. 2016; Schoeninger et al. 2001; Vincent 1985), food processing techniques such as pounding are receiving growing consideration (Crittenden and Schnorr 2017). Previous work has provided clear use wear evidence for plant-processing in Oldowan archaeological assemblages (Lemorini et al. 2014) and highlighted the significance of percussion tools used to process baobab fruit (Marchant and McGrew 2005). Here, we contribute to the discussion by providing the first 3D 360° morphometric data on use

wear of baobab pounding tools used by contemporary foragers, the Hadza of Tanzania. While the Hadza are by no means a representation of the Paleolithic past, they do offer a unique opportunity to explore the ways in which food processing techniques like pounding might leave an archaeological trace. It is our hope that systematic observation and description of these traces will allow us to better understand the function of pounding tools in the archaeological record and, in turn, the diet of our ancestors.

Morphometry has been applied for years to investigate use wear in artifacts. Variables such as roughness or fractal dimensions have been measured using confocal and profilometry data (e.g. Anderson et al., 1998; Stemp and Stemp, 2001, 2003; Evans and Donahue, 2008; Stemp et al., 2013, 2015). Most recently, GIS techniques have been employed to analyse use wear traces through surface morphometry of laser scanner data (Caruana et al., 2014; Benito-Calvo et al., 2015) allowing spatial patterns and micro-morphometric changes of use wear to be defined (de la Torre et al., 2013, Benito-Calvo et al., 2017). GIS allows computation of several morphometric indices and produces fast and accurate maps that are useful for identifying and quantifying use wear. Nevertheless, most of this software computes morphometric indices from 2.5D data (e.g. raster Digital Elevation Models, Caruana et al., 2014, Benito-Calvo et al., 2015), where the Z dimension is treated mostly as an attribute rather than as an independent coordinate. These limitations do not allow for 3D 360° analyses of the pieces, and every stone face must be processed separately. This work applies novel 3D 360° techniques to point clouds acquired directly from a laser scanner and photogrammetry in order to study the morphometric characteristics and alterations derived from baobab processing, using pounding stone tools of the same raw material. Multivariate statistical exploratory analysis is applied to the collected data for a robust understanding of the resulting use wear on artefacts.

2. Study Population

The Hadza are a population of semi-nomadic hunter-gatherers living in a 4000km^2 area around the shores of Lake Eyasi in a savanna mosaic environment in Northern Tanzania, East Africa (Marlowe 2010). Of the total population size, which numbers approximately

1000 individuals, around 150 individuals continue to practice a predominantly hunting and gathering way of life. This means that for large portions of the year, the bulk of their diet is derived from wild foods (Berbesque and Marlowe 2009; Crittenden 2016; Marlowe 2010). While no human population in Africa relies exclusively on wild foods any longer, these few remaining bush-dwelling Hadza consume few domesticated cultigens and spend significant amounts of time engaging in food collection and processing (Blurton Jones 2016). Those living in the bush consume a diverse diet composed of a wide variety of plant foods, an extensive array of bird species, small- to large-size game, and the larvae and honey of both stingless and stinging bees (Marlowe et al. 2014). Plant products include several types of berries, figs, drupes, legumes, several species of tubers (underground storage organs), and fruit from the baobab tree (*Adansonia digitata*).

Baobab fruit, known as "n//obabe" by the Hadza, is consumed throughout the year and comprises approximately 14 % of the annual diet (Crittenden 2016). The fruit has an inedible hard outer shell that accounts for approximately half of the total weight of the fruit (Nour et al., 1980). The inside of the fruit contains approximately 15 – 20 seeds which are covered with dry, white, chalky pulp. The inside of the fruit is either consumed directly out of the shell (discarding the hard seeds inside the pulp) or pounded into a flour, removing the seed husks by winnowing on the surface of small piece of animal hide (Figure 1). Pounding is done by anvil alone, without the use of hammer. The pounding stones are selected by the women prior to use and can remain in circulation for several months or years. They are often left at the pounding site for general use – by both women and children, the primary processors of baobaob fruit (Crittenden et al. 2013).

3. Methodology

3.1. Materials

Four stones used for baobab processing were collected from female Hadza foragers during January 2015 by ANC and SVL (Table 1). The stones were in use at the time of

collection and typical of the pounding stones used to process baobab fruit. All stones were collected from residents of one bush camp, Sengeli, where the majority of the diet during data collection was composed of wild plant foods, game animals, and honey (see Crittenden et al. 2017 for discussion of dietary interviews). The stones were then washed, photographed, and 3D scanned for digital analysis. Based on interviews of the foragers who provided the pounding stones, stones #1, 2, and 4 were in use for less than one week prior to data collection and stone #3 was in use for several months. Each stone was provided by a different forager and, like all baobab pounding stones, were used communally by all female foragers at the pounding site located in camp. Human Research Subjects approval for interviews and photography were obtained from the University of Nevada, Las Vegas Institutional Review Board (IRB) and all data were collected with the permission of the Tanzanian Commission for Science and Technology (COSTECH).

Stones were collected in the SW margin of the Lake Eyasi, where granitoids, gneisses, and methamorphic rocks in greenschist–amphibolite facies of the Archean Tanzanian Shield outcrop (Kabete et al., 2012). The study of stones from a single lithology (dark green amphibolites) limited the variables affecting our analysis. The only conspicuous differences between stones are due to geomorphic processes: stones #1, #3 and #4 are cobbles well rounded by fluvial processes and with no weathering features, while stone #2 is a subangular and weathered cobble, which shows initial exfoliation cracks parallel to the surface and an alteration patina with oxides on the rock surface. Therefore, we infer differences in the observed modifications to each stone are likely due to variations in baobab processing time and intensity and/or the geomorphic processes affecting the stones in the case of stone #2.

3.2. 3D data capturing

3D reconstruction of the stone tools prior to processing was performed by means of a structure-from-motion photogrammetric technique (Agisoft Photoscan 1.3.0.), since it provides a more flexible and affordable way to acquire data in the field. Stone photos were taken in the field using a conventional camera. The initial resulting point cloud

achieved an accuracy of 0.29 mm, with a mean distance between neighbouring points of around 0.2 mm. However, when aligning this model with 3D scanner data, the 3D photogrammetric data experienced a scale transformation factor of 0.86.

3D reconstruction of stone tools after processing the baobab fruit was carried out using a Next Engine laser scanner (Caruana et al. 2014; Benito Calvo et al. 2015). Stones were 360° scanned using the macro mode (accuracy ±0.1 mm), reaching a mean spatial resolution of 0.2 mm. The resulting data were exported in 3D point cloud format (Figure 2), which was also used to carry out the morphometric analysis of the post-processed stones surfaces.

3.3. 3D morphometric analysis

A critical step when analysing morphometry in 360° scanned pieces is to establish the vertical datum or origin for the elevation variable that is used to study the piece and calculate other variables (e.g. gradient or depth). A vertical datum established in a point located outside the piece would produce a variation of the elevation from one pole of the piece to the antipode (Figure 3A), instead of a variation reflecting the surficial changes, while a Z origin located in a point inside the piece (e.g. the centroid of the piece) would not accurately reflect the variations of the surficial elevation, since the pieces are not spherical (Figure 3B). In order to solve this issue, we have used an ellipsoid to create a reference vertical datum (Figure 3C). This ellipsoid was determined by generating a convex hull (Barber, 1996), which represents the smallest 3D convex surface containing all the data of the 3D point cloud. This surface joins the most external points of the pieces, defining the reference ellipsoid or vertical datum from which to calculate the elevation of the stone surface. This process was carried out for all four stone tools (Figure 2B).

The surface elevation for each piece was recalculated as the orthogonal distance between the convex hull and the point cloud representing the stone surface (Figure 3C). These elevation values were used to analyse the surface morphometry and calculate other variables including slope, curvature, roughness, depth and TPI index (Topographic Index Position index). Slope measures the steepness of a surface, and in this work, is

expressed as the gradient of the surface (i.e., the ratio change of the elevation across distance). Mean curvature was estimated as the arithmetic mean between the principal curvatures of a 3D surface in a given point (Goldman, 2005). 3D roughness was calculated following the method proposed by CloudCompare (2015), which is the distance between a given point and the best local fitting plane computed for its nearest neighbours. Mean curvature and roughness were applied considering a neighbourhood with a 0.5 mm radius. Depth was extracted directly from the difference between the convex hull and the point cloud. Depth values were used to map the 3D depressions and ridges of the surface using the TPI index (Caruana et al., 2014; Benito-Calvo et al., 2015). In this case, TPI was obtained as the difference between the depth in each point and the mean depth calculated in a radius of 5 mm around the point.

3D analysis was carried out for each stone tool. 3D mapping of morphometric variables is shown in the 3D multimedia videos (SOM videos). 3D morphometric analysis was carried out using free-access 3D software, such as MeshLab (Cignoni et al., 2008) and CloudCompare (2015). Morphometry of stone surfaces was characterized through descriptive statistics and discussed using multivariant exploratory analysis (hierarchical clustering and Principal Component Analysis, PCA), using PAST Software (Hammer et al., 2001).

3.4. 3D surface change comparison

Topographic changes in the surfaces of stones during baobab processing were investigated in one case, corresponding to face A of stone #1. This stone was photographed in the field before baobab processing, and then 3D reconstructed in the laboratory using the above mentioned photogrammetric techniques. The resulting pre-processing 3D model was compared with the post-processing 3D model, surveyed using a Next Engine laser scanner. To make these two 3D models comparable, we performed a 3D alignment of both models to adjust the scale and reference them in a common spatial coordinate system. For the latter, we used the Iterative Closest Point technique (Benito-Calvo et al., 2017). Through this technique, a reference point cloud is kept fixed, while a second point cloud is transformed (usually by a combination of translation and

rotation) to best match the reference point cloud. In this case, we chose the post-processing 3D model (surveyed with the scanner) as the reference point cloud, while the transformed point cloud was the pre-processing model (surveyed using photogrammetry). Since both 3D point clouds were generated using different techniques, we applied a variable scale during the transformation. The transformation was carried out using 500,000 comparison points, obtaining a scale transformation factor of 0.86 and a final RMS=0.199 mm, which is similar to the resolution and accuracy of both models.

Once both 3D models were aligned, changes in surface topography were measured comparing the 3D point clouds representing the stone surface before and after the baobab processing session. This comparison provided the normal distance between the two topographic surfaces for each 3D point. Following the method proposed by Benito-Calvo et al. (2017), this distance was measured using the algorithm M3C2 (Lague et al., 2013), since it provides signed and robust separation distances. This algorithm includes the estimation of a local confidence interval (95% confidence interval), to assess the position uncertainty and the registration error.

4. Results

4.1. 3D morphometry

The first step to the morphometric study of the stone tools was carried out considering their 3D surface area (S) and volume (V), which provide information regarding their general size, shape, compactness and general roughness (Table 2). Stones #2 and #4 display the highest surface area and volume measures, while stone #3 shows the lowest values in both cases (Table 2A). The lowest surface-area-to-volume ratio (S/A) was detected for stones #2 and #4 (Table 2C), indicating that both pieces are not only the biggest, but also more similar to a sphere (minimum S/A possible) than either stone #1 or #3. On the contrary, the smallest piece, stone #3, displays the highest S/A ratio (Table 2C), implying the lowest compactness which indicates the highest proportion of surface in relation to its size.

The surface area and volume of the stones relative to their respective convex hulls provide a general assessment of their roughness, as convex hulls represent the minimum possible roughness surfaces preserving only the basic shape of the stones. Surface area ratios (S_{st}/S_{ch}) with values close to 1 indicate that the stone has a low roughness, and the actual stone surface is very similar to the minimum roughness surface defined by the convex hulls. Only stone #2 has a S_{st}/S_{ch} value slightly higher than 1, indicating greater roughness for this stone, and suggesting the surface area of the stone is greater than the surface area of its minimum envelope surface. This relationship is inversely proportional considering the volume ratios (V_{st}/V_{ch}), where stone #2 shows the lowest value, since the highest roughness of its surface decreases in volume with respect to its convex hull.

Considering all the surfaces of the stones, stone #2 shows the highest mean, median, mode and maximum gradient values (Table 3), displaying a histogram that is less right skewed than stones #1, #3 and #4 (Figure 4). The gradient histograms of the latter are very similar with the main peak located around gradients of 0.03 more developed in the histogram of st#3. These relationships are similar considering the roughness and curvature parameters where the higher mean and median values belong to stone #2. Nevertheless, the highest maximum roughness is located in stone #1, and curvature modes are higher in stone #3 and stone #4 than in stone #2. The deepest and biggest depressions are located on stone #2 with mean values of -0.67 mm and minimum values of -4.23 mm, while in stones #1, #3 and #4, mean depths are situated at about -0.163—-0.175 mm and minimums are about -1.7— -1.9 mm. Depth distributions shows a bimodal pattern in most of the cases, defined by two peaks near 0 (Figure 4, Table 3). The first peak, denoted by values of 0, corresponds to the most external areas, which were used to create the convex hull defining the vertical datum. The second mode also displays values near zero (depth between -0.05—-0.02 mm), and represents the upper plains or ridges of the surface, represented in brown in Figure 5. In the stones, areas characterized by low values of gradient, curvature and roughness can be distinguished (Figure 5), which define flat, plane and polished surfaces (FPS areas). These areas are abundant in stone #3 (34%), stone #1 (32.9%) and stone #4 (31%), but are scarce in stone #2 (6.9%).

Table 3 shows the morphometric analyses carried out separately for each face and the edge of the stones. In stone #1, face A displays a smoother and flatter surface than face B. This is indicated by the lower values of gradient, roughness and curvature (Figure 5) in face A (mean, median and mode), which determine a 48.8% of FPS areas (Table 3). Such characteristics are also related to the presence of deeper depressions in face B than in face A (Figure 5). Depressions in face B reach the deepest value in stone #1 (minimum depth=-1.73 mm, Table 3), while the edge has the most irregular surface in this stone, characterised by the highest number of depressions (Table 3) and producing the deepest mean value (mean depth=-0.23 mm). The surface of the edge of stone #1 is characterised by maximum values of gradient, roughness and curvature, although mean statistics are similar to face B for roughness and curvature variables.

Differences between faces and the edge of stone #2 are less pronounced (Figure 5) and FPS areas vary between 7.9% and 5.9%. Face A shows lower gradients and curvatures than either face B or the edge, but roughness values are similar for all three. Depressions on the edge show the shallowest values of the stone (mean, median, maximum and mode, Table 3), while face B shows the deepest values (Figure 5D).

Faces A and B of stone #3 are similar (Table 3) and both display flat and smooth surfaces (FPS=41-39%) indicated by low values of gradient, curvature and roughness (Figure 5). On the contrary, the edge of stone #3 presents a rougher surface (SOM VIDEOS), denoted by an increase of the mentioned variables and a greater abundance of larger and deeper depressions (Figure 5).

On stone #4, face A is characterised by two big depressions (Figure 5D), which results in greater mean, maximum and median values for gradient, curvature and roughness (Table 3) when compared with face B. There are also more FPS areas in face B than in face A (Table 3). Depressions in face B are restricted to smaller pits (SOM VIDEOS). The roughest surface for stone #4 corresponds to the edge (SOM VIDEOS), indicated mainly by the mean and median values of the four morphometric variables and the highest percentage of depressions (Table 3). Still, the maximum values for roughness and depth are located on face A, associated with the two large depressions.

299 4.2. Surface change comparison

300 Surface changes in face A of stone #2 due to baobab processing are shown in Figure 6A.
301 This comparison displays most of the area with low absolute distance values (0—0.4
302 mm), which fall within the uncertainty range defined by the accuracy and registration
303 errors of the 3D models. However, several areas exceed this range, showing changes
304 statistically significant based on a 95% confidence interval (Figure 6A). Such significant
305 changes are located basically in the center and lower position of the face and represent
306 an abrasion of the surface defined by a mean value of -1.03 mm (maximum=-2.8 mm,
307 standard deviation=0.5 mm). These significant abrasion changes represent around 3.4%
308 of the total data analysed, and are concentrated in areas of irregular shapes with
309 maximum diameters between 0.3-29 mm.

310 Surface changes in this face have been also analysed through other morphometric
311 variables (Figure 6B). With regards to the gradient variable, most of the statistical values
312 (mean, minimum, maximum, median, mode) display a decrease from the pre-processing
313 stage (PRE) to the post-processing stage (POS) in the areas where significant abrasion
314 was detected (ST). This decrease is noticeable in the maximum values, but more
315 pronounced in the minimum gradient value which falls 86% relative to the original value
316 (0.0132). The standard deviation is the only statistical value which suffers a slight
317 increase in SC areas, from 0.077 to 0.080. This tendency is similar in the areas where no
318 significant abrasion change was detected (REST), and where also the standard deviation
319 decreases (from 0.081 to 0.073). The statistical values of the curvature variable also
320 show a general drop from the PRE to the POS stages, both in SC areas and in REST areas
321 (Figure 6B). The drop is 30-40% for the mean, median and standard deviation, 50-65%
322 for the maximum values, and 99% for the minimum values, with respect to their original
323 values. On the contrary, the curvature mode increases, changing from 0.013 m^{-1} to 0.044
324 m^{-1} in SC areas, and from 0.020 m^{-1} to 0.034 m^{-1} in REST areas. Roughness decreases for
325 all the statistical values, with the exception of the minimum roughness, which had an
326 original value of 0 mm in the PRE stage, and remains the same in the POS stage. The
327 remainder of the roughness statistics drops about 60-80%. This is also the general
328 tendency for change in the depth variable statistics (Figure 6B). In SC areas, the mean,
329 median and mode decrease in value (34-42% of the original value), the minimum

remains at 0 mm, and the maximum increases from -2.42 to -2.33 mm. In the REST areas, all the statistical values of depth increase.

5. Discussion

The results shown in Table 3 were used to analyse the morphometric relationships between the pieces through multivariant exploratory analysis (Figure 7). Hierarchical clustering of surface characteristics using Ward´s method (Hammer et al., 2001) shows a first initial group composed of stone #1 and stone #4 (Figure 7A1), which display very similar mean values of gradient, roughness, depth, curvature, percentage of depressions and FPS areas. This initial group is quite similar to stone #3, which also shows comparable morphometric characteristics. However, dissimilarities between these three pieces and stone #2 are very pronounced. This divergence is related to the highest surface topographic variability of stone #2, as indicated by the ratios S_{st}/S_{ch}, V_{st}/V_{ch} and the surface morphometric variables. This stone shows the highest values of gradient, curvature, roughness, the lowest percentage of FPS areas and the biggest and deepest depressions. The divergence of stone #2 is also clear through PCA analysis (Figure 7B). In this case, PC1 -which explains 71% of the variance- clearly separates stone #2 from the rest of the stones. Although stone #2 was used only for a few days (Table 1), this broad morphometric difference between stone #2 and the rest of the pieces is likely related to raw material differences rather than to differences use or intensity of use, given that stones #1 and #4 were also only in use for less than a week. Stone #2 is a subangular cobble affected by weathering which increases the topographic variability, while stone #1, #3 and #4 are alluvial cobbles that were rounded and smoothed by water transport prior to use in baobab processing. PC1 also shows a relationship between stone #1 and #4 (as the hierarchical clustering also indicates), which are the most similar pieces in size and shape (Figure 2), and may have been gripped and used in more similar ways during the baobab processing.

Multivariant analysis of 3D morphometric data also allows comparisons between the different areas of the stones. Hierarchical clustering of Figure 7A2 displays four clusters. A first cluster corresponds to the areas of stone #2. As mentioned above, faces and edge

of this stone show the highest topographic variability. This first cluster is related to a second group, which comprises the areas with more surface irregularities in the rest of the stones (#1, #3 and #4). These areas are the edges, which are not subject to abrasion and polishing processes during the use of the stone and as a result, preserving the original irregularities of the stones. This second group also includes face B of stone #1. This face shows high values of gradient, roughness and curvature indicating characteristics more similar to the edges than to the rest of the faces. This suggests that face B of stone #1 could have been used less than the faces of stones #1, #3 and #4, preserving topographic features similar to the edges. Although no other data is available, face B of stone #1 could be used mainly as the palm side of the stone, while face A may have been the side that mainly contacted the baobab during processing. The third and fourth clusters are distant from clusters 1 and 2, and correspond to the rest of the faces of stones #1, #3 and #4, which show smoother relief probably associated with the abrasion and polish that occurred during their use. Cluster 3 is composed by a core integrated by both faces of stones #3 (which was the most used stone over a period of several months), and at a distance, face A of stone #4. Cluster 4 includes face A of stone #1 and face B of stone #4.

PCA analysis allows discrimination between similar groups. PC1 separates clearly the areas of stone #2 from the areas of the rest of the stones, which are restricted to the left sector of the PC1-PC2 graph (Figure 7B1). In this sector, PC1 values also differentiate the edges from all other faces (including face B of stone #1). PC1 tends also identifies another group consisting of faces A and B of stone #3, face B of stone 4 and face A of stone #1. In this last group, face B occupies a very similar position. Loadings for PC1 show a strong positive coefficient of correlation (>0.9) with the statistics of gradient (mean and median), roughness (mean, median and standard deviation), mean curvature (mean, median and standard deviation); and also, a strong but negative correlation (<-0.9), with depth (mean and mode) and FPS areas (Figure 7B3). The strongest PC2 loadings correspond to the curvature mode (-0.62), the maximum depth (0.61) and the minimum curvature (0.50).

In order to study the surface evolution in the particular case of stone #2, we compared the surface of face A before and after the baobab processing. 3D alignment techniques

allow us to equal the scale and to reference both 3D models, obtaining reasonable errors which were taken into account when establishing a confidence interval for detecting and measuring significant changes. Statistically significant changes (ST areas, Figure 6) are mainly distributed in the lower central part of the face, suggesting that this was the area of more intense use, which produced a maximum surface abrasion of -2.8 mm. This loss of material in face A is related to a general decrease in the gradient, roughness and curvature variables resulting in a smoother surface. This process may not be homogenous and progressive, as shown by microscopic measurements in experimental stones used in bone pounding that indicate an alternating pattern of smoothing and roughing of stone surfaces during the course of use (Benito-Calvo et al., 2017). The depth of face depressions is also altered by baobab processing, which causes an increase in the mean depth, but a decrease in maximum depth. The increase in mean depth is explained by an increase in the area occupied by depressions due to the loss of material caused by the abrasion. However, this abrasion erodes the surface, reducing the maximum depth of the depressions relative to the surrounding surface. Overall, changes in the ST areas are large enough to suggest that use wear produced by baobab processing could be detectable in the archaeological record using macro-scale techniques.

On the other hand, in the areas where no significant changes were detected (REST areas, Figure 6), the morphometric trend of the surface seems to be similar with a general decrease in gradient, roughness and curvature and an increase in depth, suggesting that depressions became shallower due to the smoothing produced by the baobab processing. However, this last morphometric trend is tentative since no statistically significant changes were detected in REST areas.

This methodology provides an objective way to define quantitative 3D signatures for percussion activities, which can be applied to other lithics and percussion issues in order to create a database of morphometric signatures. Pounding features are identified through morphometric parameters and values which can be assessed with statistics. This provides an unprecedented way to reduce uncertainty associated with the visual identification of use wears. In addition, surficial changes observed in the plant processing stones can be used to understand how the surfaces of archaeological pieces

bearing the same traces were prior to pounding and, therefore, allow reconstruction of the abrasion process in the archaeological record.

6. Conclusions

This paper explores the potential of 3D techniques to study the use wear features of pounding stone tools. Here, we develop and present new methods for the 360° morphometric analysis of artefacts from 3D point clouds captured directly from laser scanners or photogrammetric methods. In applying these methods to study pounding stone tools used by Hadza people to process baobab, we have obtained several morphometric variables which map the topographic variability of stone surfaces. Multivariant exploratory analysis of these data through hierarchical clustering and PCA analysis has reduced uncertainty and subjectivity in the data analysis, revealing that the artefacts and the different faces of each stone can be grouped according to the initial characteristics of the raw material and uses. Differences in stone tools of the same raw material allow detection of the effect of variable geomorphic processes on the stones prior to processing, as well as intensity of human use, which can be investigated for the complete stone tools or for different areas of the same stone tool.

Surface comparison conducted on 3D models surveyed before and after the baobab processing has shown that the abrasion pattern suffered in one of the stones is characterized by significant changes near the center lower position of the stone. This abrasion produced a general smoothing of the surface and an increase of the area of depressions but reduced the maximum measured depth of the depressions. Although the methodology is also applicable to confocal 3D microscopic level, the scale of the observed changes suggest that these traces should be detectable in the archaeological record through 3D macro-scale techniques.

The work presented here provides evidence that 3D morphometric analyses of stone tools used by contemporary foragers is a promising endeavor that requires further exploration and could potentially reveal the 3D morphometric signatures and abrasion patterns of plant processing through pounding techniques. It is critical to focus

attention on tools that may have been used for processing raw plant foods, as the dates for the first controlled use of fire remain contentious (Sandgathe and Berna 2017), as well as dates for the first stone butchery tools (Harmand et al., 2015). Plant foods, which were essential to the diets of our earliest hominin ancestors, remain key contributors to the diets of all sub-tropical foraging populations. Increasing our knowledge of stone percussive activities by contemporary foragers will further our understanding of non-thermal processing techniques in the archaeological record, potentially shedding new light on the importance of plant foods to early hominin subsistence strategies.

The method we have presented here is broadly applicable to any archaeological site. However, the next stage of this research should be the application of this technique to characterise the signatures produced by other types of pounding and grinding activities on a variety of raw materials, while controlling for the length and types of use (pounding vs grinding). With a diverse understanding of the various traces produced on pounding stones, we can better elucidate the distinct ways our ancestors used these tools at the archaeological sites from which they are recovered.

7. Acknowledgements

We would like to thank the Hadza for their research participation and the Tanzanian Commission for Science and Technology (COSTECH) for research approval. Funding by the European Research Council (Starting Grant, 283366) is acknowledged. 3D analysis was conducted using the hardware facilities and Agisoft Photoscan software of the Laboratory of Digital Mapping and 3D Analysis (CENIEH).

8. References

Anderson, P., Astruc, L., Vargiolu, R., Zahouani, H., 1998. Contribution of quantitative analysis of surface states to a multi-method approach for characterizing plant processing traces on flint tools with gloss, in: Facchini, D., Palma di Cesnola, A., Piperno, M., Peretto, C. (Eds.), Functional Analysis of Lithic Artefacts: Current State of 459 the Research. Proceedings of the XIII Congress (Forli, 8-14 September 1996). UISPP. ABACO, Forli, pp. 1151–1160.

Arroyo, A., Hirata, S., Matsuzawa, T., de la Torre, I., 2016. Nut Cracking Tools Used by Captive Chimpanzees (Pan troglodytes) and Their Comparison with Early Stone Age Percussive Artefacts from Olduvai Gorge. PLOS ONE 11, e0166788. doi:10.1371/journal.pone.0166788

Barber, C.B., Dobkin, D.P., Huhdanpaa, H.T., 1996. The Quickhull algorithm for convex hulls. ACM Transactions on Mathematical Software 22, 469–483.

Benito-Calvo, A., Arroyo, A., Sánchez-Romero, L., Pante, M., De La Torre, I., 2017. Quantifying 3D micro-surface changes on experimental stones used to break bones and their implications to the analysis of Early Stone Age pounding tools. Archaeometry in press.

Benito-Calvo, A., Carvalho, S., Arroyo, A., Matsuzawa, T., de la Torre, I., 2015. First GIS Analysis of Modern Stone Tools Used by Wild Chimpanzees (*Pan troglodytes verus*) in Bossou, Guinea, West Africa. PLoS ONE 10, e0121613. doi:10.1371/journal.pone.0121613

Caruana, M.V., Carvalho, S., Braun, D.R., Presnyakova, D., Haslam, M., Archer, W., Bobe, R., Harris, J.W.K., 2014. Quantifying Traces of Tool Use: A Novel Morphometric Analysis of Damage Patterns on Percussive Tools. PLoS ONE 9, e113856. doi:10.1371/journal.pone.0113856

Cignoni, P., Corsini, M., Ranzuglia, G., 2008. MeshLab: an Open-Source 3D Mesh Processing System. ERCIM News 73, 45–46.

CloudCompare, 2015. CloudCompare. 3D point cloud and mesh processing software Open Source Project.

Crittenden, A.N., 2016. Ethnobotany in evolutionary perspective: wild plants in diet composition and daily use among Hadza hunter-gatherers, in: Hardy, K., Kubiak-Martens, L. (Eds.), Wild Harvest: Plants in the Hominin and Pre-Agrarian Human Worlds. Oxford University Press, Oxford, pp. 319–340.

Crittenden, A.N., Conklin-Brittain, N.L., Zes, D.A., Schoeninger, M.J., Marlowe, F.W., 2013. Juvenile foraging among the Hadza: Implications for human life history. Evolution and Human Behavior 34, 299–304. doi:10.1016/j.evolhumbehav.2013.04.004

Crittenden, A.N., Schnorr, S.L., 2017. Current views on hunter-gatherer nutrition and the evolution of the human diet. Am J Phys Anthropol 162, 84–109. doi:10.1002/ajpa.23148

de la Torre, I., Benito-Calvo, A., Arroyo, A., Zupancich, A., Proffitt, T., 2013. Experimental protocols for the study of battered stone anvils from Olduvai Gorge (Tanzania). Journal of Archaeological Science 40, 313–332. doi:10.1016/j.jas.2012.08.007

de la Torre, I., Hirata, S., 2015. Percussive technology in human evolution: a comparative

approach in fossil and living primates, Philosophical Transactions of the Royal Society of London B: Biological Sciences. Royal Society, London.

Evans, A.A., Donahue, R.E., 2008. Laser scanning confocal microscopy: a potential technique for the study of lithic microwear. Journal of Archaeological Science 35, 2223–2230.

Goldman, R., 2005. Curvature formulas for implicit curves and surfaces. Computer Aided Geometric Design 22, 632–658. doi:10.1016/j.cagd.2005.06.005
Hammer, Ø., Harper, D.A.T., Ryan, P.D., 2001. Paleontological Statistics Software Package for Education and Data Analysis. Palaeontologia Electronica 4, 9.

Hardy, K., Martens, L.K., 2016. Wild Harvest: Plants in the Hominin and Pre-Agrarian Human Worlds. Oxbow Books.

Harmand, S., Lewis, J.E., Feibel, C.S., Lepre, C.J., Prat, S., Lenoble, A., Boes, X., Quinn, R.L., Brenet, M., Arroyo, A., Taylor, N., Clement, S., Daver, G., Brugal, J.-P., Leakey, L., Mortlock, R.A., Wright, J.D., Lokorodi, S., Kirwa, C., Kent, D.V., Roche, H., 2015. 3.3-million-year-old stone tools from Lomekwi 3, West Turkana, Kenya. Nature 521, 310–315.

Henry, A.G., Brooks, A.S., Piperno, D.R., 2014. Plant foods and the dietary ecology of Neanderthals and early modern humans. Journal of Human Evolution 69, 44–54. doi:10.1016/j.jhevol.2013.12.014

Jones, N.B., 2016. Demography and Evolutionary Ecology of Hadza Hunter-Gatherers, Cambridge Studies in Biological and Evolutionary Anthropology. Cambridge University Press.

Kabete, J.M., Groves, D.I., McNaughton, N.J., Mruma, A.H., 2012. A new tectonic and temporal framework for the Tanzanian Shield: Implications for gold metallogeny and undiscovered endowment. Ore Geology Reviews 48, 88–124. doi:10.1016/j.oregeorev.2012.02.009

Lague, D., Brodu, N., Leroux, J., 2013. Accurate 3D comparison of complex topography with terrestrial laser scanner: Application to the Rangitikei canyon (N-Z). ISPRS Journal of Photogrammetry and Remote Sensing 82, 10–26. doi:10.1016/j.isprsjprs.2013.04.009

Lemorini, C., Plummer, T.W., Braun, D.R., Crittenden, A.N., Ditchfield, P.W., Bishop, L.C., Hertel, F., Oliver, J.S., Marlowe, F.W., Schoeninger, M.J., Potts, R., 2014. Old stones' song: Use-wear experiments and analysis of the Oldowan quartz and quartzite assemblage from Kanjera South (Kenya). Journal of Human Evolution 72, 10–25. doi:10.1016/j.jhevol.2014.03.002

Marchant, L.F., McGrew, W.C., 2005. Percussive technology: chimpanzee baobab smashing and the evolutionary modeling of hominid knapping, Stone knapping: the necessary conditions for a uniquely hominid behavior, in: Roux, V., Bril, B. (Eds.), Stone

Knapping: The Necessary Conditions for a Uniquely Hominin Behaviour. McDonald Institute for Archaeological Research, Cambridge, pp. 341–352.

Marlowe, F., 2010. The Hadza: Hunter-gatherers of Tanzania, Origins of human behavior and culture. University of California Press.
Marlowe, F.W., Berbesque, J.C., 2009. Tubers as fallback foods and their impact on Hadza hunter-gatherers. Am. J. Phys. Anthropol. 140, 751–758. doi:10.1002/ajpa.21040

Marlowe, F.W., Berbesque, J.C., Wood, B., Crittenden, A., Porter, C., Mabulla, A., 2014. Honey, Hadza, hunter-gatherers, and human evolution. Journal of Human Evolution 71, 119–128. doi:10.1016/j.jhevol.2014.03.006

Mora, R., de la Torre, I., 2005. Percussion tools in Olduvai Beds I and II (Tanzania): Implications for early human activities. Journal of Anthropological Archaeology 24, 179–192. doi:10.1016/j.jaa.2004.12.001

Nour, A.A., Magboul, B.I., Kheiri, N.H., 1980. Chemical composition of baobab fruit (Andasonia digitata L.). Tropical Science 22, 383–388.

Sandgathe, D.M., Berna, F., 2017. Fire and the Genus Homo: An Introduction to Supplement 16. Current Anthropology 58, S165–S174. doi:10.1086/691424
Schnorr, S.L., Crittenden, A.N., Henry, A.G., 2016. Impact of Brief Roasting on Starch Gelatinization in Whole Foods and Implications for Plant Food Nutritional Ecology in Human Evolution. Ethnoarchaeology 8, 30–56. doi:10.1080/19442890.2016.1150629

Schoeninger, M.J., Bunn, H.T., Murray, S.S., Marlett, J.A., 2001. Composition of Tubers Used by Hadza Foragers of Tanzania. Journal of Food Composition and Analysis 14, 15–25. doi:10.1006/jfca.2000.0961

Stemp, W.J., Lerner, H.J., Kristant, E.H., 2013. Quantifying microwear on experimental mistassini quartzite scrapers: Preliminary results of exploratory research using LSCM and scale-sensitive fractal analysis. Scanning 35, 28–39.

Stemp, W.J., Lerner, H.J., Kristant, E.H., 2013. Quantifying microwear on experimental mistassini quartzite scrapers: Preliminary results of exploratory research using LSCM and scale-sensitive fractal analysis. Scanning 35, 28–39.

Stemp, W.J., Stemp, M., 2003. Documenting Stages of Polish Development on Experimental Stone Tools: Surface Characterization by Fractal Geometry Using UBM Laser Profilometry. Journal of Archaeological Science 30, 287–296. doi:10.1006/jasc.2002.0837

Stemp, W.J., Stemp, M., 2001. UBM Laser Profilometry and Lithic Use-Wear Analysis: A Variable Length Scale Investigation of Surface Topography. Journal of Archaeological Science 28, 81–88. doi:10.1006/jasc.2000.0547

Vincent, A.S., 1985. Plant Foods in Savanna Environments: A Preliminary Report of Tubers Eaten by the Hadza of Northern Tanzania. World Archaeology 17, 131–148.

Captions for tables and figures

Table 1. Use and location of the stone tools.

Table 2. Surface area (S) and volume (V) dimensions and ratios of pounding tools. A) Surface area and volume of pounding stone tools (st) #1 to #4. B) Surface area and volume of convex hulls (ch) #1 to #4. C) Surface-area-to-volume ratio (S/V) for pounding stone tools (st) and convex hulls (ch). D) Surface area and volume ratios comparing pounding tools with their respective convex hulls.

Table 3. Basic statistics of gradient, mean curvature, roughness and depth variables calculated in stones #1 to #4 for the complete surface (all), the surface of face A, the surface of face B, and the surface of the edge. FPS: flat, plane and smooth areas defined by the lowest values of gradient, curvature and roughness.

Figure 1. A Hadza woman pounds baobab seeds into flour, which is then winnowed with a piece of animal hide

Figure 2. Pounding tools 3D models surveyed after the baobab processing using laser scanner. A) Shaded point clouds captured using 3D laser scanner NextEngine. B) Convex hulls calculated for each pounding tool.

Figure 3. Different methods to establish the vertical datum or elevation data origin used to calculate the 3D 360° morphometric variables. A) Vertical datum located in a point outside of the piece. B) Vertical datum located in a point inside the piece. C) Vertical datum located in a spheroid representing the minimum convex hull of the piece.

Figure 4. Histograms of gradient, mean curvature, roughness and depth values for the complete surface of stones #1 to #4.

Figure 5. Four of the morphometric variables calculated for stones #1 to #4. A) Gradient. B) Mean curvature. C) Roughness. D) Depth. 3D spatial distribution of these morphometric variables can be observed in the SOM videos.

Figure 6. Surface changes for pounding stone #2 (face A) detected after the baobab processing. A) Changes and significant abrasion areas calculated using the normal distance between the 3D point clouds surveyed before and after the baobab processing. Normal distance was estimated by means of the M3C2 algorithm (Lague et al., 2013; D= 1 mm, d= 1 mm). B) Morphometric variables measured in face A before (PRE) and after (POS) the baobab processing, for the areas where a statistically significant abrasion was detected (SC), and for the rest of the surface (REST).

Figure 7. Multivariate exploratory analysis considering the morphometric variables of Table 3. A) Hierarchical clustering dendogram for stones #1 to #4 (A1), and their faces and edges (A2), applying the Ward´s method (Hammer et al., 2001). B) Principal component analysis, displaying the scatter plot for principal components PC1 and PC2 (B1), scree plot (B2) and loading for PC1 (B3). Colour hulls: areas of the same stone. Gray hulls: relationships between areas of different stones

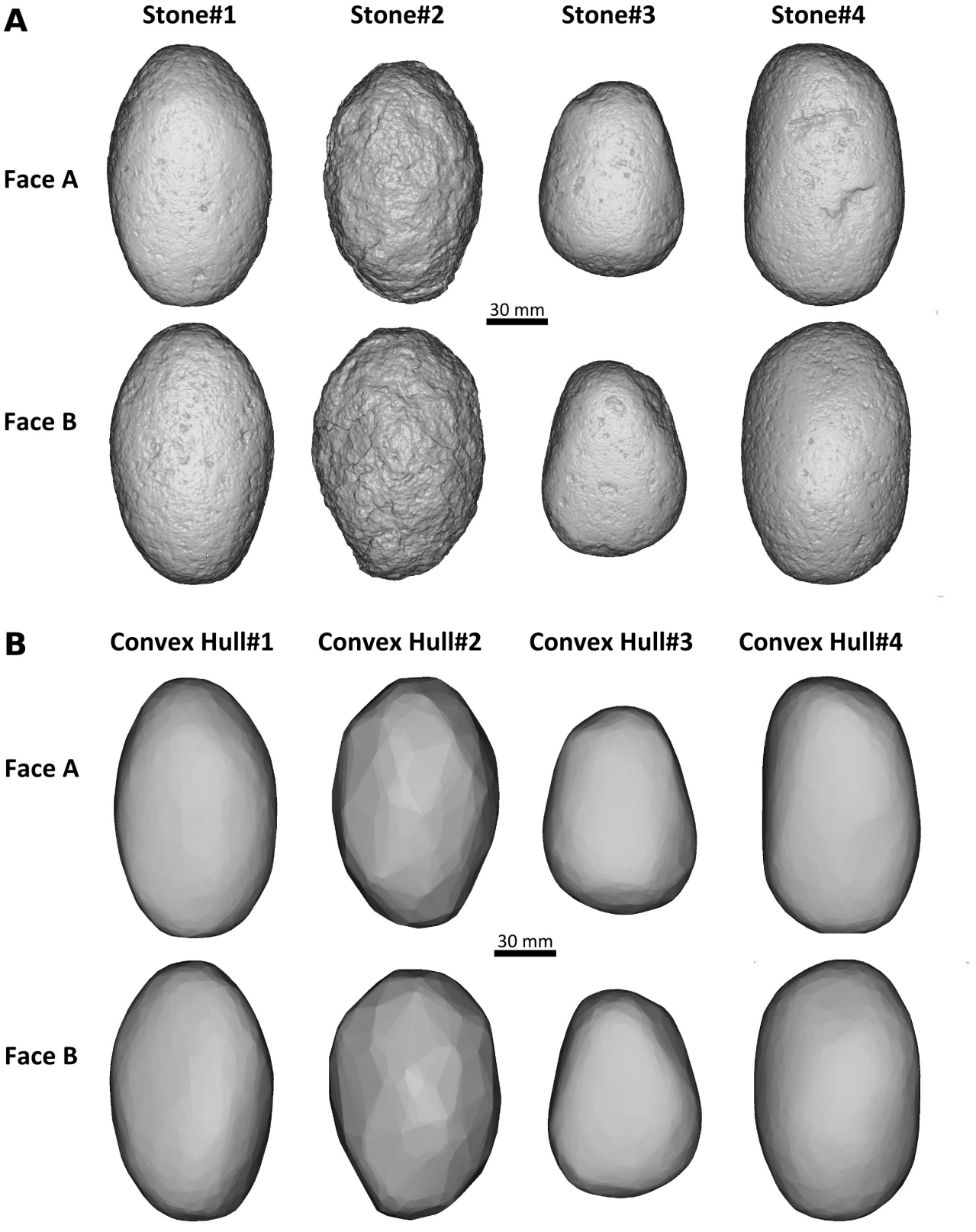
A
Stone#1
Stone#2
Stone#3
Stone#4
Face A
30 mm
Face B
B
Convex Hull#1
Convex Hull#2
Convex Hull#3
Convex Hull#4
Face A
30 mm
Face B

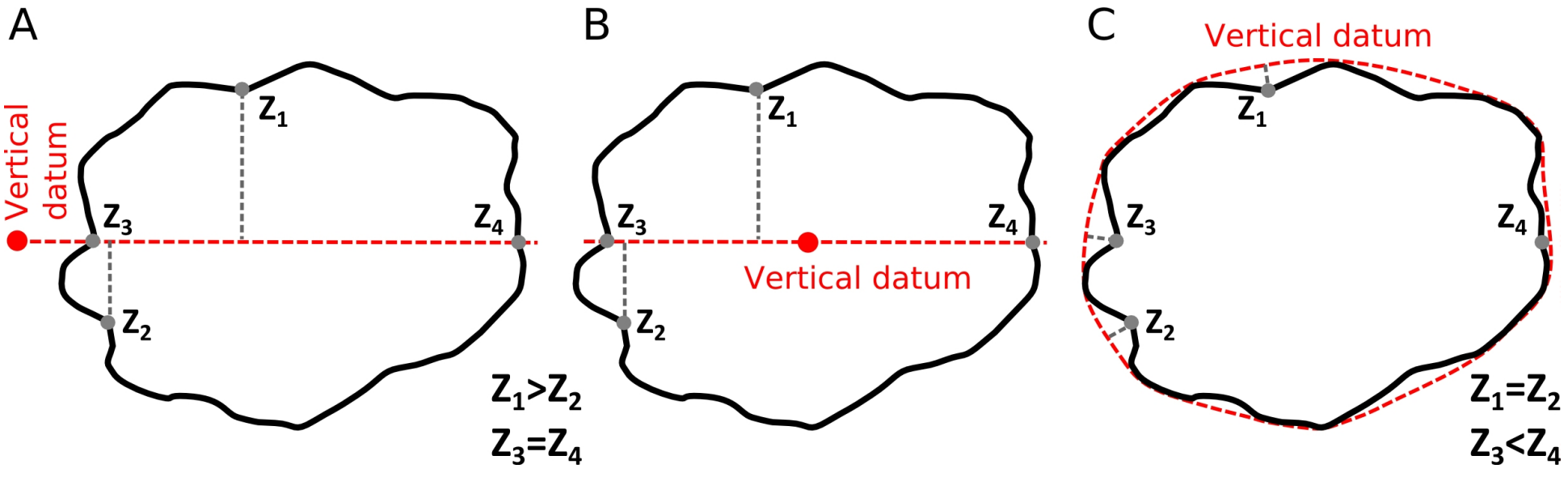
A
Vertical datum
Z1
Z3
Z4
Z2
Z1>Z2
Z3=Z4
B
Z1
Z3
Z4
Vertical datum
Z2
C
Vertical datum
Z1
Z3
Z4
Z2
Z1=Z2
Z3<Z4

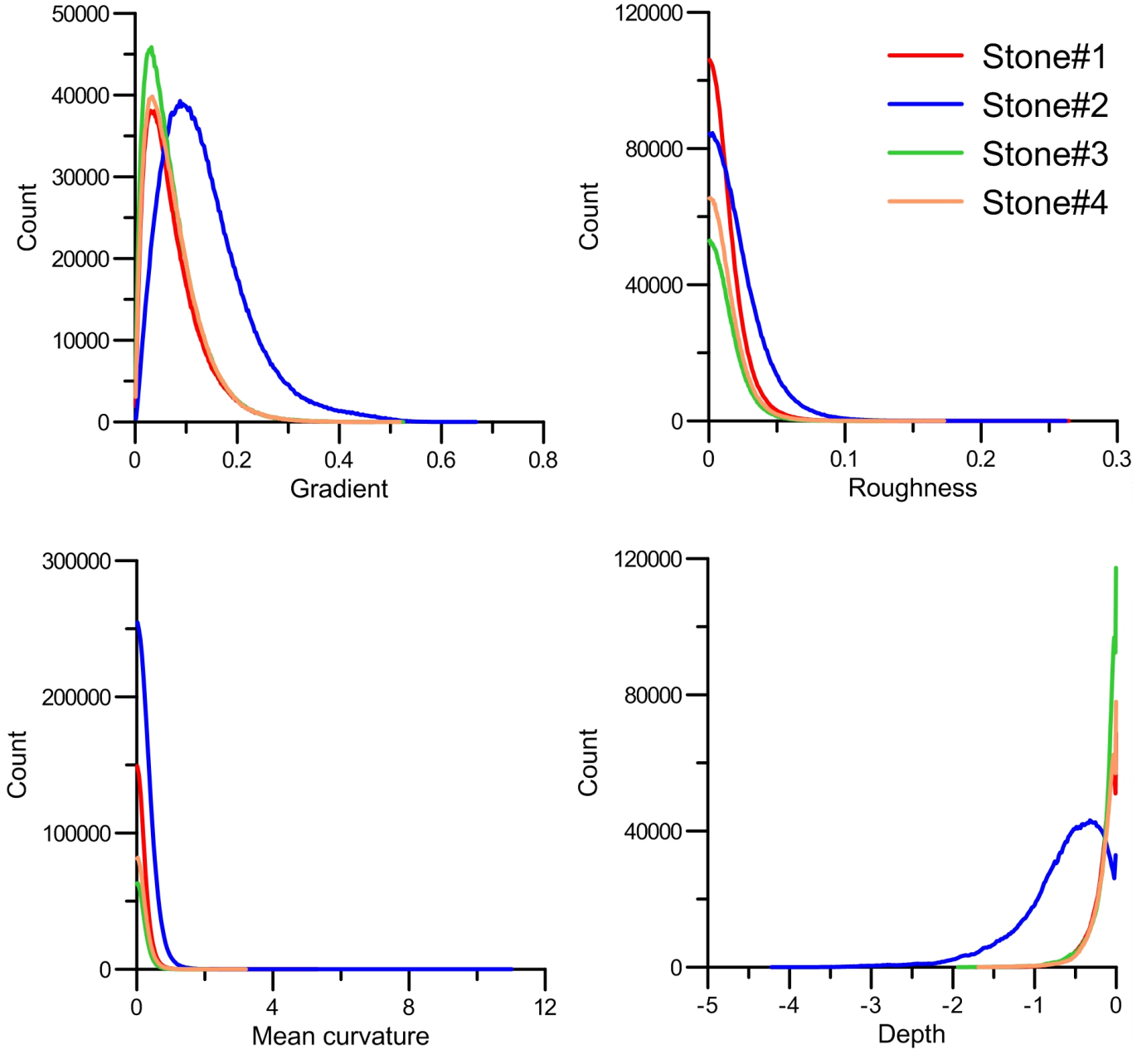
Count
Gradient
Roughness
Mean curvature
Depth
Stone#1
Stone#2
Stone#3
Stone#4

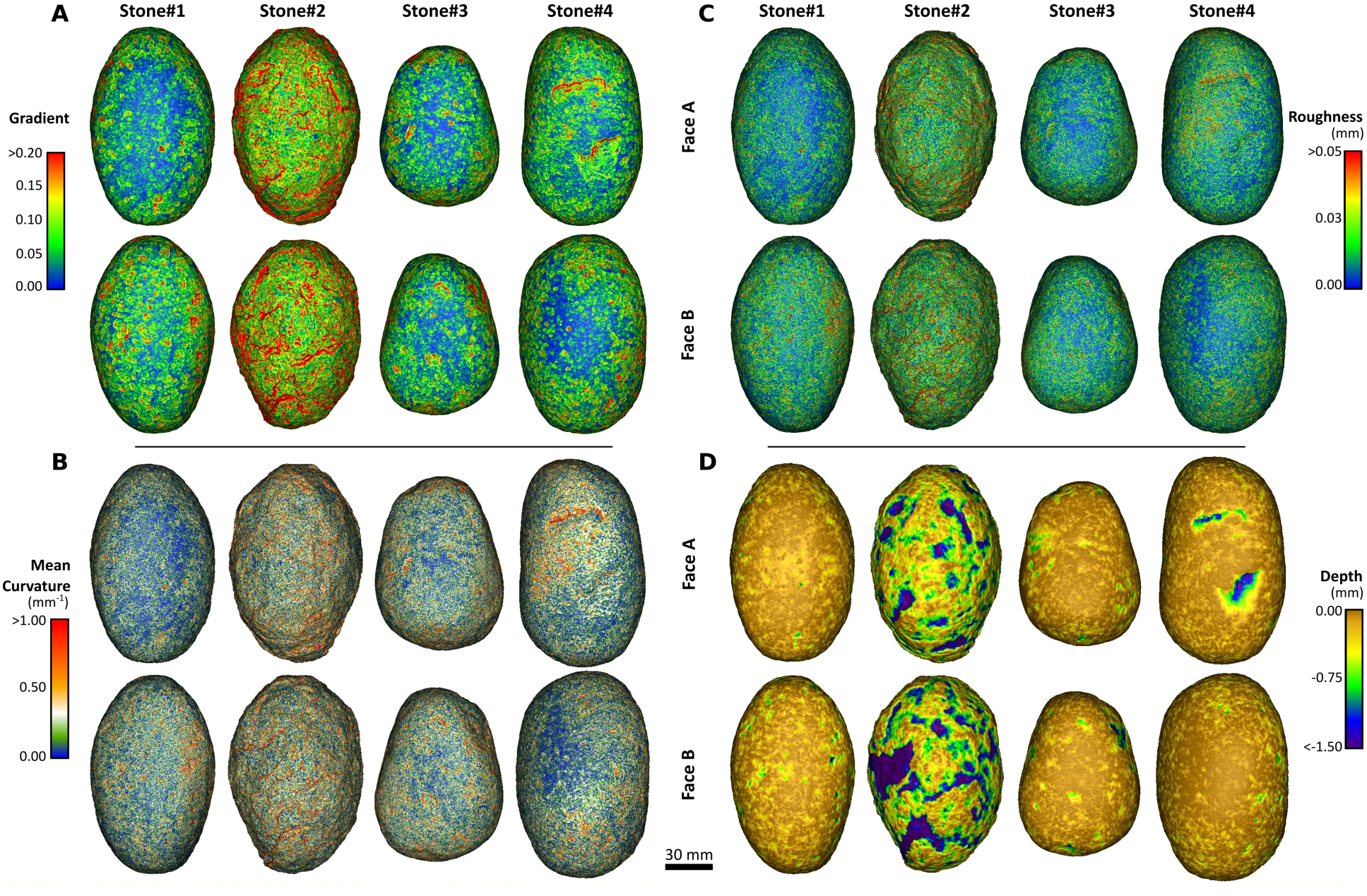
A
Stone#1
Stone#2
Stone#3
Stone#4
Gradient
>0.20
0.15
0.10
0.05
0.00
C
Face A
Face B
Roughness
(mm)
>0.05
0.03
0.00
B
Mean
Curvature
(mm-1)
>1.00
0.50
0.00
D
Depth
(mm)
0.00
-0.75
<-1.50
30 mm

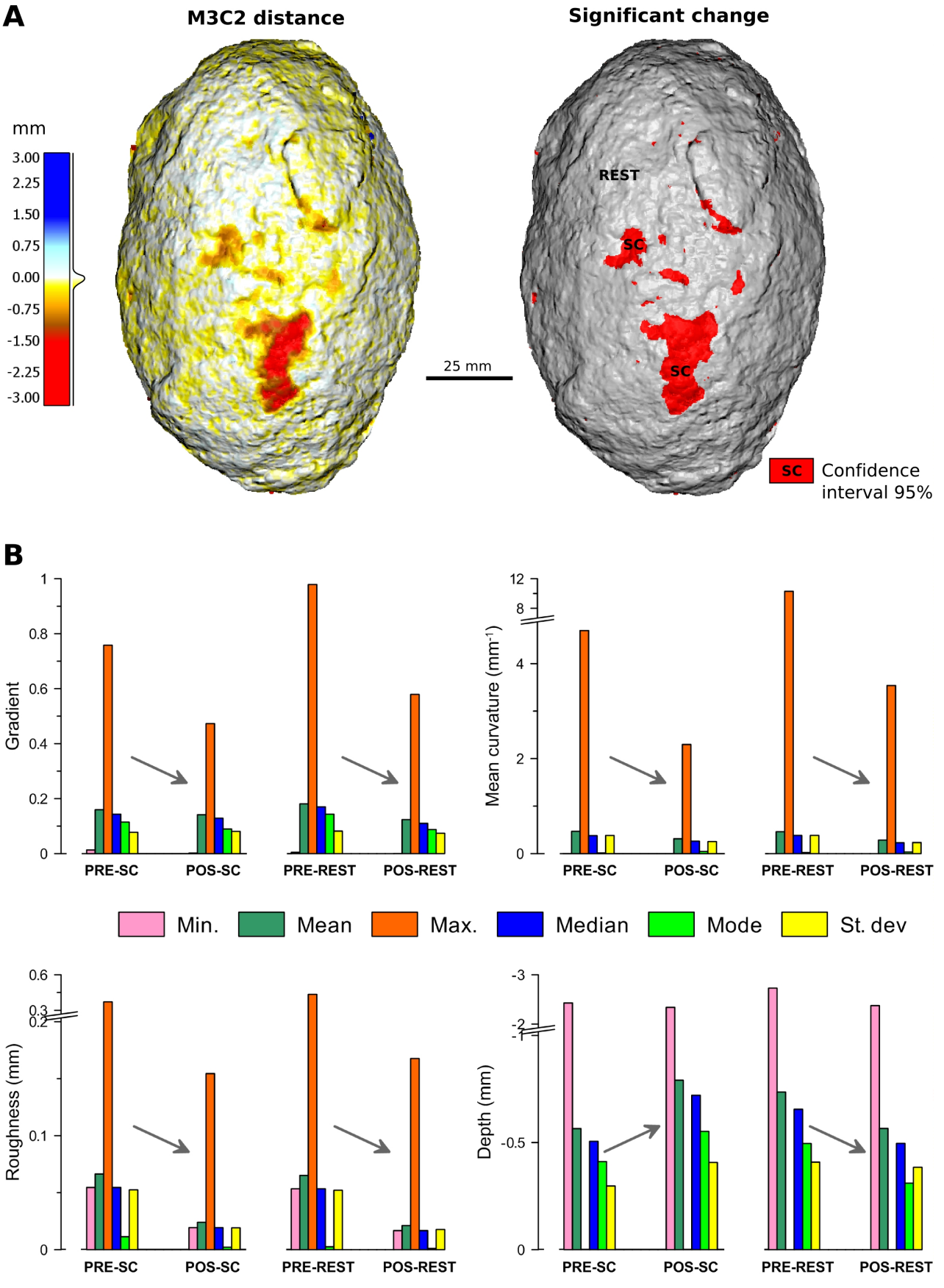
A
M3C2 distance
Significant change
mm
3.00
2.25
1.50
0.75
0.00
-0.75
-1.50
-2.25
-3.00
25 mm
REST
SC
SC
SC
Confidence interval 95%
B
Gradient
Mean curvature (mm-1)
Roughness (mm)
Depth (mm)
PRE-SC
POS-SC
PRE-REST
POS-REST
Min.
Mean
Max.
Median
Mode
St. dev

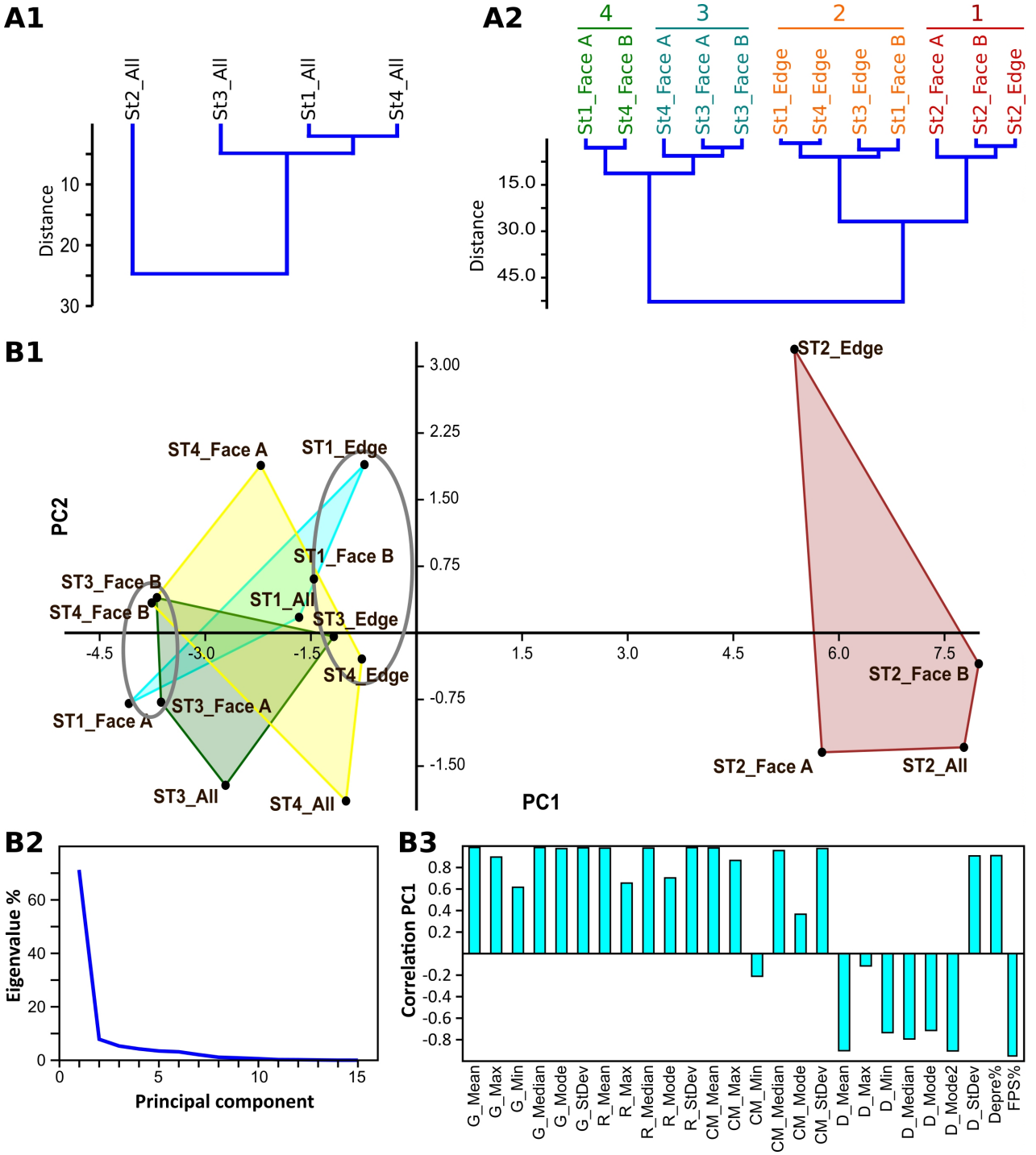
A1
St2_All
St3_All
St1_All
St4_All
Distance
10
20
30
A2
4
3
2
1
St1_Face A
St4_Face B
St4_Face A
St3_Face A
St3_Face B
St1_Edge
St4_Edge
St3_Edge
St1_Face B
St2_Face A
St2_Face B
St2_Edge
Distance
15.0
30.0
45.0
B1
PC2
PC1
ST4_Face A
ST1_Edge
ST1_Face B
ST3_Face B
ST1_All
ST4_Face B
ST3_Edge
ST4_Edge
ST1_Face A
ST3_Face A
ST3_All
ST4_All
ST2_Edge
ST2_Face B
ST2_Face A
ST2_All
3.00
2.25
1.50
0.75
-0.75
-1.50
-4.5
-3.0
-1.5
1.5
3.0
4.5
6.0
7.5
B2
Eigenvalue %
Principal component
0
20
40
60
0
5
10
15
B3
Correlation PC1
0.8
0.6
0.4
0.2
-0.2
-0.4
-0.6
-0.8
G_Mean
G_Max
G_Min
G_Median
G_Mode
G_StDev
R_Mean
R_Max
R_Median
R_Mode
R_StDev
CM_Mean
CM_Max
CM_Min
CM_Median
CM_Mode
CM_StDev
D_Mean
D_Max
D_Min
D_Median
D_Mode
D_Mode2
D_StDev
Depre%
FPS%